Soft Tissues' Loadings on Healthy Knee at Different Physiological Flexions: A Coupled Experimental–Numerical Approach

Boris Dousteyssier, Jérôme Molimard, Chafiaa Hamitouche, Woo-Suck Han and Eric Stindel

Abstract In this study, the movement of climbing a step is decomposed in 4 EOS images. A patient-dependent 3D model of the knee is then created from MRI, and several numerical simulations are carried out according to the experimental boundary conditions (force and flexion angle), so as to ensure the global knee mechanical equilibrium. To validate this patient-specific model, its bony structure is confronted with the EOS images once the mechanical equilibrium is reached. This model gave us an estimation of the stress in the ligaments for every flexion angle as well as a pressure map on the cartilages.

Introduction

Knee osteoarthritis is one of the major causes of disability in older adults. According to a study conducted in the United Kingdom and the Netherlands on a population of 55 y.o. and more, 25% declared having chronical and persistent knee pain (Peat et al. 2001). Osteoarthritis is the combined effect of degradation of the cartilage, thickening of the subchondral bone and new bone formation on the edges of the cartilages. The main clinical diagnosis tool for osteoarthritis is the radiography, with effects being apparent on X-ray images: joint space narrowing for the cartilage destruction, variation of the signal intensity for the thickening of the

B. Dousteyssier · J. Molimard · W.-S. Han (✉)
CIS-EMSE, Ecole Nationale Supérieure Des Mines de Saint-Etienne,
42023 Saint Etienne, France
e-mail: han@emse.fr

B. Dousteyssier · J. Molimard · W.-S. Han
INSERM U1059, SAINBIOSE, 42023 Saint Etienne, France

B. Dousteyssier · J. Molimard · W.-S. Han
Université de Lyon, 69000 Lyon, France

B. Dousteyssier (✉) · C. Hamitouche (✉) · E. Stindel
Laboratoire de Traitement de l'Information Médicale, INSERM UMR 1101,
29609 Brest, France

subchondral bone and the bone formation is directly seen. The knee degradation and the associated pain when developing osteoarthritis are strongly related not only to the pressure on the cartilage, but also to the knee stability and to the subsequent loadings on the ligaments. Numerical models of the knee can help us evaluate both of these in a daily situation for the knee and understand the osteoarthritis phenomenon. Some knee joint models already exist in the literature. Some authors proposed knee models without any flexion (Pena et al. 2006; Donahue et al. 2002). But those models as incomplete as they may be only represent a small part of the knee functionality, and most likely not the part that is significant in the deterioration of the knee. Other authors have introduced knee flexion, for example by directly controlling active muscular groups (Marouane et al. 2015). But the pressure applied on the articulations may be questioned, given the difficulty to assess the physiological level of the forces used to perform the flexion. On another paper, the knee flexion is modelled by using a full displacement-controlled model (Zhong et al. 2011). In this case the uncertainties of the bone positioning may lead to high variations in the cartilage pressure and ligament loads. It especially removes the link between the two phenomena, separating the cartilages and the ligaments by the bones that are completely controlled by the user.

Here our approach is coupled, using both the experimental data by the means of medical imaging and a finite element model to have a physiological representation of the knee and its solicitations at a given flexion angle. In order to do so, a geometrical model is created from the MRI, with which a numerical simulation of an experimental setup is conducted. The experimental setup modelled is the EOS imaging of the movement decomposition of climbing a step. The EOS is a low-dose X-ray system (Wybier and Bossard 2013) and thus is already used in order to diagnose knee osteoarthritis. Its acquisition area allows upright position during the acquisition, as well as some room to instal a step. An added benefit of the climbing a step movement is that the flexion angle of the knee is higher than during the gait movement (Kaufman et al. 2001). The goal of this approach, a numerical simulation of an experimental setup, is to create a model that will be validated by comparing its numerical results with the EOS data. This model will reveal the roles of the ligaments during the knee flexion and give pressure maps on the cartilages.

Method

EOS Acquisition

A healthy volunteer (24 y.o., BMI = 26.23 kg/m^2) undergoes an EOS imaging of the right knee decomposing the movement of climbing a step. The height of a step ranges from 130 to 180 mm or even 210 mm for stiff stairs. For practical reasons, this study was conducted for a step of 150 mm. Between each acquisition, a 50 mm thick block is added under the foot of the volunteer until the step height of 150 mm is reached. During the whole procedure, a weighting scale is positioned under the
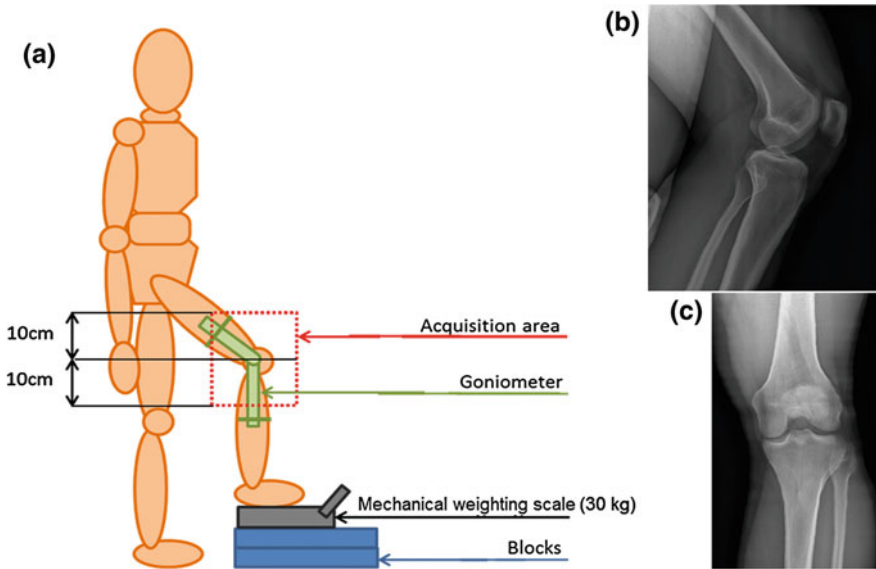
Fig. 1 **a** Schematics of the EOS acquisition setup—side view. **b** Sagittal scan of the knee at 55° of flexion—i.e., 10 cm height step. **c** Matching frontal scan of the knee

foot of the volunteer for him to maintain a constant load of 30 kg. This ensures us the most homogenous boundary conditions possible on the knee at different flexion angles for the following numerical simulations. This load has been chosen to be the most comfortable to maintain while being immobile during the whole acquisition procedure. Even though the EOS acquisition is rather quick, approximately 10 seconds per flexion angle, a lighter load has proven to be difficult to control at lower flexion angles and respectively a heavier one is near impossible for higher flexion angles. The data obtained is 5 sagittal and 5 frontal scans of the knee hard tissues at the flexion angles of 0°, 40°, 55°, and 70°. Those images give access to the physiological position of the bones at those specific angles of flexion. The schematics of this acquisition and examples of data obtained are shown in Fig. 1.

3D Geometric Model

The 3D geometrical model of the bones and cartilages used in the simulations to be as complete and physiologic as possible, it is segmented from three different MRI stacks of the volunteer's knee. The MRI modalities used are SPIN echo for the cruciate ligaments insertions, SPIN echo with fat saturation for the lateral ligaments insertions and the cartilages and finally gradient echo for the bones of the articulation. These three MRI stacks has to be fitted one on the other in order for all the different segmented parts to be coherent in the model. The software used for the segmentation is AVISO® (FEI, Hillsboro, United States). The segmented model is

then smoothed with a low-pass filter using the toolbox GIBBON® for MATLAB® (MathWorks, Natick, United States) and meshed with HARPOON® (Sharc, Manchester, United Kingdom). Those different steps in the making of the geometrical model can all be source of uncertainties and so a special care is taken so that the patient-specific aspect of this model is not lost during the process. The study on the tools used for the model creation has been presented previously (CMBBE-2015) and only a brief recall is given here for the reader's comprehension. It shows that the error between the final geometry and the initial data is less than a millimetre, which is a very good precision because it corresponds to the width of two voxels in the MRI raw data.

Finite Element Modelling

In the present model, only the tibia and the femur are considered. The patella is not included because it can be neglected for the passive stability-oriented analysis. The bones being a lot more rigid than any other materials in the analysis, they are considered as rigid bodies. The cartilages are viscoelastic tissues; however this analysis being static, the viscosity has no impact in the equilibrium of the model. And thus they are modelled as single-phase linear elastic and isotropic material with an elastic modulus of $E = 12$ MPa, and a Poisson ratio of $v = 0.45$ (Yao et al. 2006). The cartilages are tied to their respective bones, and the contact between the two cartilages is defined as "hard", meaning that no intersection whatsoever is allowed between the two surfaces in contact. A friction coefficient of $\mu = 0.08$ has been taken. Finally the ligaments modelled are the anterior cruciate ligament (ACL), the posterior cruciate ligament (PCL), the lateral collateral ligament (LCL), and the medial collateral ligament (MCL). They are modelled as truss elements working in tension only, and pined on the segmented insertions area. As truss elements they are considered as transversely isotropic. The cross-sectional areas for the ligaments are 42, 60, 18, 25 mm^2 for respectively the ACL, PCL, LCL and MCL. Longitudinally, they are modelled as hyperelastic materials following the stress/strain curve given by Gardiner and Weiss (2003). In the standing position all ligaments have an initial tension of 100 N (Oh et al. 2014), this initial tension has been adjusted to the differences in strain of the different flexion angles and then transferred accordingly. The inferior insertion point of the LCL is on the fibula. But since the bones are modelled as rigid bodies, the fibula does not have any other relevant role in this simulation. So to lighten our model, we simply add an element on the tibia in order to reach the correct LCL insertion on the fibula. The geometrical model is shown in Fig. 2. It is composed of 43,500 linear elements (tetrahedron, hexahedron and prism). During the convergence analysis, it is noticed that the number of elements in the bones or ligaments matters little due to their modelling. The bones modelled as rigid bodies only require enough element for their contact surface to be smooth. Otherwise, it would create stress concentration on the cartilages on the tied nodes. The ligaments taken individually are in a very
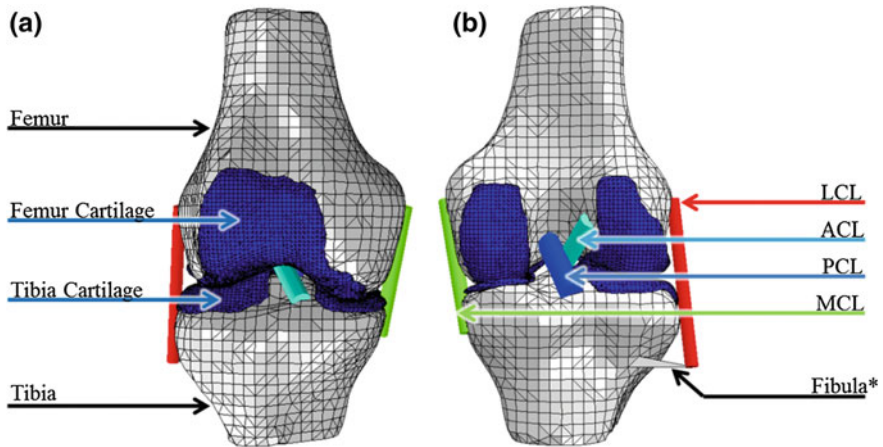
Fig. 2 Finite element model of the knee joint. **a** Front view. **b** Back view. *Asterisk* element added on the Tibia to reach the physiological inferior insertion point of the LCL

simple state. Since no contact are defined other than their insertion areas, they work as a hyperelastic spring. For those reasons most of the elements are in the cartilages, the most critical parts of this model: they make for 29,500 of the elements.

Numerical Simulations

The simulations are carried on ABAQUS® (Dassault Systèmes, VélizyVillacoublay, France). The goal of each simulation is to respect the experimental conditions of the EOS data acquisition. In order to do so, the initial bone position of this model is fitted on the physiological positions from the EOS data for the four different flexion angles. We managed to fit the 3D model on two 2D EOS images so as to check the contour of a projection of the 3D model, then to fit and to compare it with the segmented contour of the EOS images. The method used is based on the Iterative Closest Point (Zhang et al. 2016) in order to fit the two contours, and use the simplex method to find the best match between the possible bone contours from the model with the segmented contours of the EOS images. The fitting precision obtained is 1 mm on the two projected planes and 0.5° along the bone axis. The specifics of the algorithm and an example of contour fitting are shown in Fig. 3.

Once the bones are in their physiological positions for each flexion angles, an intersection between the cartilage of the femur and those of the tibia can be noticed. The numerical simulation is composed of the following steps: (1) slightly move the tibia downward to remove this intersection, while keeping the femur blocked, (2) put the boundary conditions of the experimental setup, (3) obtain the global knee mechanical equilibrium by applying the same load as the experimental
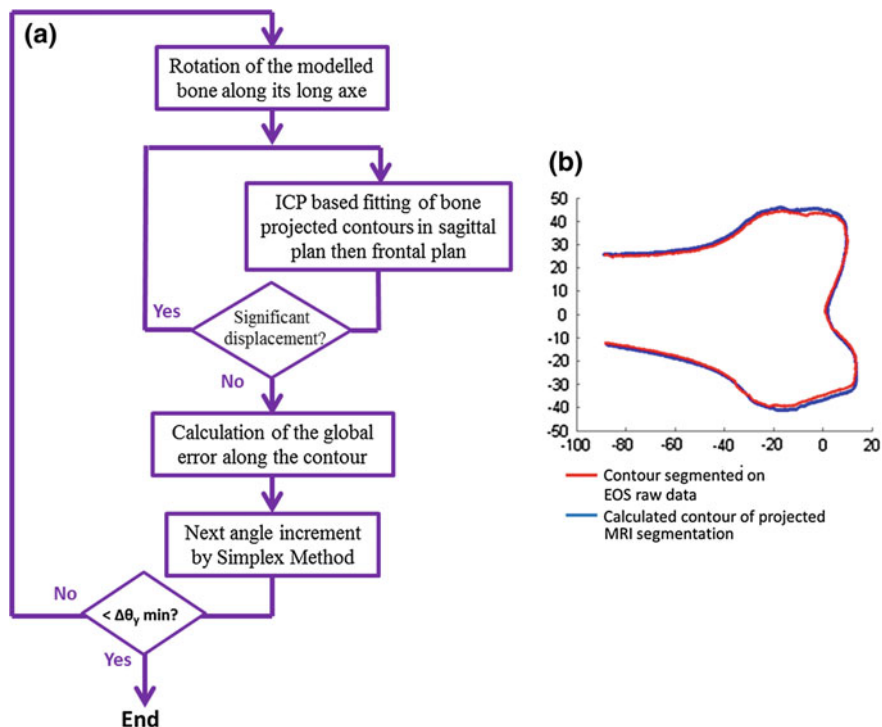
Fig. 3 **a** Fitting algorithm of a 3D model on two 2D projections. **b** Example of a contour comparison: frontal plan of the femur at a 0° flexion angle

setup. All along the analysis, the femur is fixed in space; all degrees of freedom of the tibia are initially locked too. The first step consists in translating the tibia along its axis until there is no more intersection between the cartilages. At this point the contact between the cartilages is implemented and the force on the tibia is added: 300 N along its axis. Then all degrees of freedom are released except the rotation in the sagittal plane that is the flexion angle. The FEA is carried out until the global knee mechanical equilibrium. Once achieved, the equilibrium position of the tibia is compared with its initial position, directly linked to the experimental data, to assess the validity of the model. All steps of the FEA are summarized in Fig. 4.

Results

Tibia Position

The first result sought is the tibia position. Comparing this position with the initial EOS data ensured that the model and the global equilibrium reached are indeed
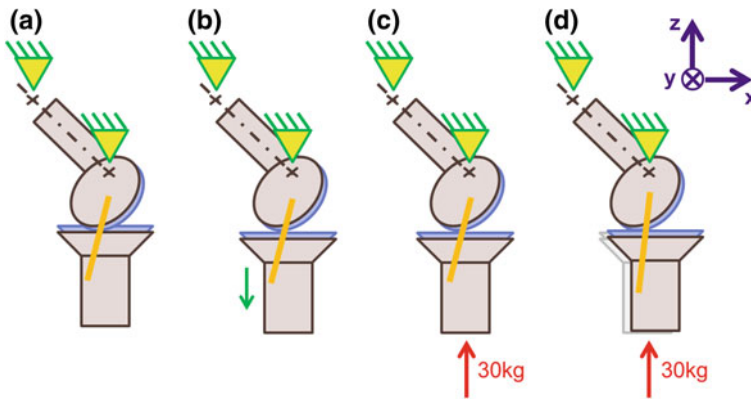
Fig. 4 FEA steps: **a** initial position, **b** removal of the cartilages intersection, **c** addition of the contact and experimental boundary conditions, **d** global knee mechanical equilibrium
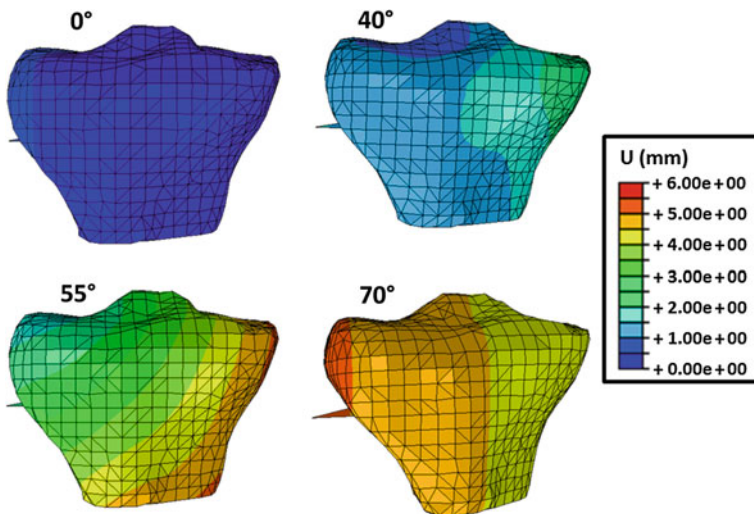

Fig. 5 Position distance of each node to their counterpart on the experimental data

physiological. On Fig. 5, we can see the distance of each node from their experimental position for the four flexion angles studied, 0°, 40°, 55° and 70°. The simulation at a flexion angle of 0° shows an insignificant distance between the simulation and the experiment for every points of the tibia. The maximum distance observed stands only at 0.7 mm. For the flexion angle of 40°, we can also observe that this distance is very small: for 97% of the nodes, their FEA position is at most 2 mm apart from their EOS position. The greatest distance observed is 2.66 mm. With the gradient of displacement, we can observe that the difference in positions is due to a rotation along the bone axis, measured at 2.6°. On the 55° flexion angle

simulation, the distances vary from 1.75 to 5.24 mm, but less than 4 mm for 81% of the nodes. Once again those differences are due to a rotation, this time mainly on the frontal plane, measured at 3.7°. Finally for the flexion angle of 70°, the distances observed are between 4.0 and 5.2 mm. Here the principal cause of this difference is an anterior translation, the displacement component along this axis ranging from 3.8 to 5.0 mm.

Cartilages Pressure Map

In Fig. 6 are shown the different pressure maps for the four simulations. We can see that in each case the pressure is rather balanced on the two condyles, with a slight overpressure on the external condyle. Furthermore the point of maximum pressure follows the line of contact described in other studies (Shandiz et al. 2016). The maximum pressure for the different flexion angles are 3.43, 5.34, 5.89 and 5.23 MPa for respectively 0°, 40°, 55° and 70°. We can also notice that the area under pressure is a little more spread for the flexion angle of 0°, and more focused for 40°, 55° and 70°.
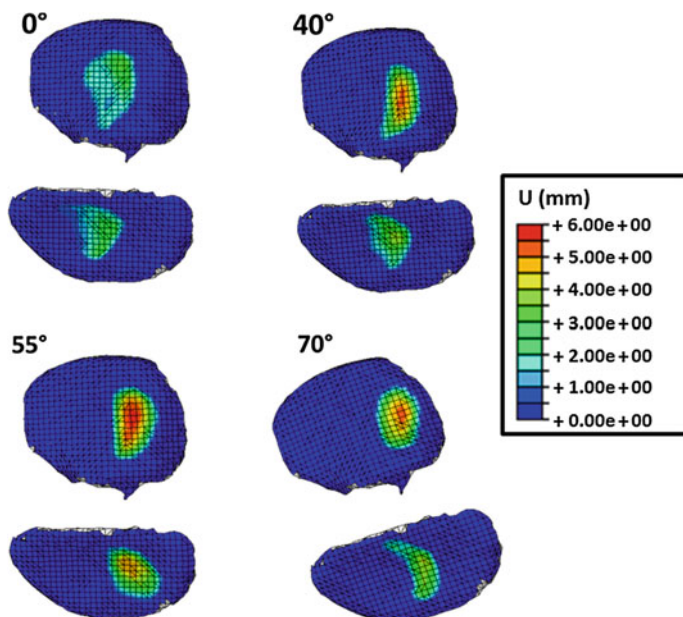

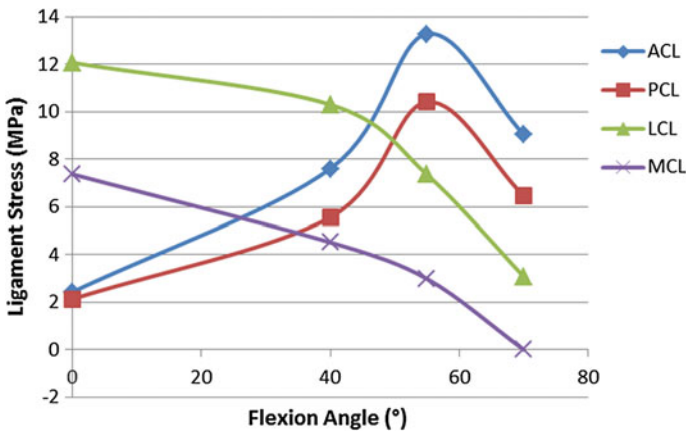**Fig. 6** Pressure map on tibia cartilages after global knee equilibrium

Fig. 7 Stress in the ligaments depending on the flexion angle

Ligament Stress

Finally the last result that is focused on is the ligaments stress repartition depending on the flexion angle. As shown in Fig. 7, we can see that at the lowest flexion angle the collateral ligaments withstand more stress, with their maximum stress at a flexion angle of 0° being 12.07 and 7.37 MPa for the lateral and medial collateral ligaments respectively. Then the stress steadily decreases as the flexion angle increases until the LCL reaches 3.07 MPa and the MCL is totally relaxed for the 70° flexion angle. At 40° flexion angle, the stress is balanced between the different ligaments, but for higher flexion angles it is focused in the cruciate ligaments. The stress in the cruciate ligaments starts lightly at 2.43 and 2.13 MPa for the anterior and posterior cruciate ligaments respectively in the standing position to reach a peak at the 55° flexion angle with stresses of 13.27 and 10.41 MPa.

Discussion

Boundary Conditions and Material Properties

This first patient dependant knee joint model simulate the climbing a step movement. It decomposes it in several quasi static situations at flexion angles ranging from 0° to 70°. It is built combining the EOS imaging system and an MRI acquisition of the volunteer. The MRI data is the base of the geometrical model and the EOS data brought the physiological bone positions at those different flexion

angles. This model focuses on the passive stability of the knee and so the modelled parts of the knee are the bones (femur and tibia as rigid bodies), the cartilages (as isotropic elastic and linear elements) and the ligaments (ACL, PCL, MCL and LCL as hyperelastic truss elements). In this first simulation the influence of the linear elements of the cartilages is not yet assessed. A future step will be to use quadratic elements and see if the results differ enough to justify the added simulation time. The contact between the cartilages is defined as hard (with no intersections) with a friction coefficient $\mu = 0.08$. This friction coefficient is rather high but it is the closest possible to the literature [$\mu = 0.02$ (Mow et al. 1997)] in order for all the simulation to reach equilibrium. The limiting simulation is for a flexion angle of 55°. In this simulation the static equilibrium cannot be reached as the tibia seams to slide on the femur. This is a clear limitation of the model that will be addressed in the future. During the numerical simulation, the cartilage intersection due to the bone positioning is removed, the experimental boundary conditions are added and the global knee equilibrium is reached. On average, each simulation took approximately 1100 s of CPU time, which took around 30 min of wall clock time. Even though the positions of the bones are accessible with the EOS images, those simulations cannot be executed simply by controlling the displacement of the bones. When they are done this way most of the high flexion angles simulations do not reach equilibrium: the elements in the cartilages are too much distorted and the simulation end prematurely. At low flexion angle the simulations do reach equilibrium but the results, especially the pressure maps, are not reliable. The resulting force on the tibia is calculated as high as 3200 N, which is more than 10 times the expected result. We can also see that there is a strong imbalance between the pressures on the two condyles: for example at 40° flexion angle, the maximum pressure is 8.7 MPa on the exterior condyle and 5.9 MPa on the interior one.

FE Model Validation by Bone Position

After the creation of the FE model and once the simulations are complete, the first step is to come back to the experimental data, i.e., EOS images, in order to make sure that this model is physiologically correct. The physiological position of the bones in the knee joint given by EOS imaging is compared with their position obtained by FEA after the global knee equilibrium is reached with the same boundary conditions. The numerical results have a good agreement with the EOS images. For the two lowest flexion angles they are as good as they can get: the precision of the fitting of the 3D model on the EOS raw data is precise within 1 mm, meaning that after the equilibrium, the difference on the tibia (only moving part of the model) of 2 mm is within that precision range of EOS data's precision. Thus in that distance interval the difference between the simulation and the experimental data can equally be explained by (1) the simulation equilibrium missing the physiological position by a tiny amount or (2) our position

measurement of the experimental data that could slightly be improved. As a reminder, this precision corresponds to only two voxels in the data gathered on the MRI. Therefore, the simulation of the standing leg with a maximal distance of 0.7 mm is totally in its physiological position and the simulation at a 40° flexion angle, with 97% of its nodes at less than 2 mm of their experimental counterparts, is almost perfectly aligned with the experimental data. For the 55° flexion angle simulation, the final position of the bones is still very good; 81% are at most at twice the precision range, making it an acceptable error of position. However, this model can be questioned for the simulation at the flexion angle of 70°. In this state, every node is at least at 4 mm of their aimed position. But in this particular case, we underlined that this distance is mostly due to an anterior translation of the tibia. At this flexion angle, the tibia seams to start to slip more than its physiological movement given by EOS images. The height of a step varying from 130 to 210 mm, we conducted the entire protocol for a fifth flexion angle, for the case of a high step. An EOS image with a 200 mm high step has been taken and the corresponding numerical simulation is launched. But it could not achieve equilibrium, as the minimal time increment is not enough however small it is. On the incomplete result we can observe an anterior translation, similar to the simulation at the 70° flexion angle. It is very likely that at this high flexion angle the tibia starts to slip on the femur and that the ligaments are not enough to stabilise the modelled knee joint.

Model Shortcomings

This model may prove to be lacking some stability tools, like the menisci that would directly be in the way of such a translation. Considering that, adding the menisci is the next step for the development of this model. In two of the simulations, we could also notice a slight rotation of the bone along its long axis. This may be due to the lack of contact between the ligaments and their surroundings. As the model is, nothing stops the cruciate ligaments to intersect each other, whereas physiologically they would twist one on the other and impede this rotation. However, this kind of rotation is very small and to attend to it may not be essential considering how this contact may make the model more complex. Adding contact conditions between the ligaments and the bone can also slightly change the way the lateral collateral ligament would work; adding a small lever arm on its tibia intersection and maybe making the whole knee joint a bit more stable. Once again the changes would prove to be to smalls to make this addition in the model a priority. Finally, the higher the flexion angle, the more the active stability may be impactful. This model focuses in the passive stability but maybe some active stability is necessary for a global equilibrium at higher flexion angle, especially in this case are the knee is loaded. As the patella can be segmented on EOS images, a future model could involve a fitted patella, fixed in space as the femur, linked to the tibia with the patellar tendon.

Pressure Maps and Ligament Stress

This first model, even incomplete, still shows some physiological behaviour. Beside the good bone position, we can see on the pressure maps that the points of highest pressure are in agreement with the contact path described by Shandiz et al. (2016). The pressure is rather well balanced between the two condyles, as expected from a healthy knee. We can separate two kind of pressure map along the flexion; first the standing leg and second every bent knee. In the first case, at the 0° flexion angle we can see that the area under pressure is more spread than the other case and that the maximum pressure is a lot lower, standing at 3.43 MPa. Whereas for the flexion angles of 40°, 55° and 70° it is more focused with a maximum pressure around 5.5 MPa. This dichotomy in the pressure maps is explained by the contact surface of the femur condyles. At a 0° flexion angle the curvature angle of the contact surface is more obtuse, allowing a better stability for the knee in the standing position, making holding it for a long period of time more comfortable. For the other flexion angles, this curvature angle is more acute, making the flexion movement easier, and this movement smoother in general. Moreover, the slight overpressure on the external condyle showcases the different purpose of the two condyles: the internal condyle guiding the flexion while the external sustain a higher load. The stress in the ligaments also highlights the different functions of the ligaments. The collaterals ligaments guarantee the knee joint stability in extension while the cruciate take over in flexion. We can notice that usually it is the medial collateral ligament that is more loaded than the lateral (Dufour and Pillu 2007); in this case it is the opposite because the volunteer suffer from a light varus (4.5°). A maximum stress in the cruciate ligaments along rotation is recorded near 55°. It is due to the complex kinematics of the femur on the tibial plateaux, mixing translation and rotation. Indeed, this value remains qualitative, considering the angular discretization step.

Conclusion

In order to study on the question of knee degradation and pain when developing osteoarthritis, related to both the pressure on the cartilages and the knee stability, a knee joint model was created. We proposed a mixed approach, both using medical imaging (MRI, EOS X-ray system) and force platform in conjunction with a FE model. The goal was to obtain pressure maps on the cartilages of the knee and the stress sustained by its ligaments during a daily activity.

The movement of climbing a step was chosen for its higher flexion angle of the knee joint. A FE model was created, focusing on passive stability and recreating an experimental setup: the decomposition in 4 static EOS images of the movement of climbing a step. In order to do so, a geometrical model of the volunteer's knee was fitted on the physiological bone position obtained on the EOS images. Once the

initial parasitic intersection removed, the experimental boundary conditions were added and the numerical simulation is carried on until a global knee mechanical equilibrium was reached. Then the simulated position of the bones could be compared with the experimental one, and we obtained pressure maps on the cartilages and the stress in the ligaments for this controlled situation.

Thanks to this method allowing to compare the FE model with the experimental data, here the bone positions, we know when we can be confident in the results obtained and when we have to be cautious. Here this very simplified model showed that for low flexion angles it could achieve a global knee mechanical equilibrium that is perfectly physiological. Even with every degree of freedom released, except the flexion angle, the numerical simulation for the flexion angles of 0° and 40° has a very good concordance with the measured experimental data. For higher flexion angles the results were promising. The FE simulation for the flexion angle of 55° was still close to the experimental data, with most of its nodes within 4 mm of their experimental counterpart. And for the flexion angle of 70° we can notice that only one movement has to be taken care of: an anterior translation.

This model will have to be completed in order to achieve a better stability, mostly for the higher flexion angles. We are currently working on the addition of the menisci in this model. We hope that this will allow us to obtain a lower friction coefficient and address to the anterior translation in the numerical simulation of the 70° flexion angle. After that the next step would be the modelling of the ligaments as the 3D parts with contacts that they are, and check their influence on our current results. As long as possible we will keep focusing on a passive stability-oriented model, in order to control each of its aspect.

References

Donahue TLH et al (2002) A finite element model of the human knee joint for the study of tibio-femoral contact. J Biomech Eng 124(3):273–280

Dufour M, Pillu M (2007) Biomécanique fonctionnelle: membres, tête, tronc. Rappels anatomiques, stabilité, mobilités, contraintes

Gardiner JC, Weiss JA (2003) Subject-specific finite element analysis of the human medial collateral ligament during valgus knee loading. J Orthop Res 21(6):1098–1106

Kaufman KR et al (2001) Gait characteristics of patients with knee osteoarthritis. J Biomech 34(7):907–915

Marouane H, Shirazi-Adl A, Hashemi J (2015) Quantification of the role of tibial posterior slope in knee joint mechanics and ACL force in simulated gait. J Biomech 48(10):1899–1905

Mow VC, Ateshian GA (1997) Lubrication and wear of diarthrodial joints. Basic Orthop Biomech 2:275–315

Oh KJ, Park WM, Kim K, Kim YH (2014) Quantification of soft tissue balance in total knee arthroplasty using finite element analysis. Comput Methods Biomech Biomed Eng 17(14):1630–1634

Peat G, McCarney R, Croft P (2001) Knee pain and osteoarthritis in older adults: a review of community burden and current use of primary health care. Ann Rheum Dis 60(2):91–97

Pena E et al (2006) A three-dimensional finite element analysis of the combined behavior of ligaments and menisci in the healthy human knee joint. J Biomech 39(9):1686–1701

Shandiz MA, Boulos P, Saevarsson SK, Yoo S, Miller S, Anglin C (2016) Changes in knee kinematics following total knee arthroplasty. Proc Inst Mech Eng Part H J Eng Med 230: 265–278

Wybier M, Bossard P (2013) Musculoskeletal imaging in progress: the EOS imaging system. Joint Bone Spine 80(3):238–243

Yao J et al (2006) Stresses and strains in the medial meniscus of an ACL deficient knee under anterior loading: a finite element analysis with image-based experimental validation. J Biomech Eng 128(1):135–141

Zhang C et al (2016) Robust iterative closest point algorithm with bounded rotation angle for 2D registration. Neurocomputing 195:172–180

Zhong Y et al (2011) Stress changes of lateral collateral ligament at different knee flexion with or without displaced movements: a 3-dimensional finite element analysis. Chin J Traumatol 14(2):79–83